Biochimica et Biophysica Acta, 984 (1989) 301–312
Elsevier

BBAMEM 74559

Polarized infrared absorption of Na^+/K^+-ATPase studied by attenuated total reflection spectroscopy

U.P. Fringeli [2,3], H.-J. Apell [1], M. Fringeli [3] and P. Läuger [1]

[1] *Department of Biology, University of Konstanz, Konstanz (F.R.G.),* [2] *Institute of Physical Chemistry, University of Vienna, Vienna (Austria) and* [3] *Laboratory for Physical Chemistry, ETH Zürich, Zürich (Switzerland)*

(Received 10 March 1989)

Key words: ATPase, Na^+/K^+-; Infrared reflection spectroscopy; Attenuated total reflection

Na^+/K^+-ATPase can be isolated from the outer medulla of mammalian kidney in the form of flat membrane fragments containing the enzyme in a density of 10^3–10^4 protein molecules per μm^2 (Deguchi et al. (1977) J. Cell. Biol. 75, 619–634). In this paper we show that these membrane fragments can be bound to a germanium plate coated with a phospholipid bilayer. With this system infrared spectroscopic studies of the enzyme have been carried out using the technique of attenuated total reflection (ATR). At a coverage of the lipid surface corresponding to 30–40% of a monolayer of membrane fragments, characteristic infrared bands of the protein such as the amide I and II bands can be resolved. About 24% of the NH-groups of the peptide backbone are found to be resistant to proton/deuterium exchange within a time period of several days. Evidence for orientation of the protein with respect to the supporting lipid layer is obtained from experiments with polarized light, the largest polarization effects being associated with the $-COO^-$ band at 1400 cm^{-1}. Experiments with aqueous media of different ionic composition indicate that the average orientation of transition moments changes when K^+ in the medium is replaced by $Tris^+$ or Na^+.

Introduction

The sodium-potassium pump (Na^+/K^+-ATPase) in the plasma membrane of animal cells carries out uphill transport of sodium and potassium ions at the expense of free energy of ATP hydrolysis [1–9]. The Na^+/K^+-ATPase may be isolated from biological membranes by detergent solubilization in the form of functionally active oligomers of composition $\alpha\beta$ or $\alpha_2\beta_2$ [10]. The α subunit binds ATP and is transiently phosphorylated during the catalytic cycle. The function of the β subunit, a glycoprotein containing about 20% carbohydrate by mass, is not precisely known; it probably acts as a receptor for the integration and orientation of the α subunit in the membrane [11]. The amino-acid sequence of both subunits of Na^+/K^+-ATPase from kidney have been determined from their cDNA sequence [12–14]; the α subunit of the sheep kidney enzyme contains 1016, the β subunit 302 amino-acid residues. The Na^+/K^+-ATPase is a transmembrane protein consisting of a large polar part protruding into the cytoplasm, a membrane-spanning portion which is thought to consist of several hydrophobic α-helices, and a small polar part facing the extracellular side [12–24].

Information from spectroscopic experiments on the secondary and tertiary structure of the Na^+/K^+-ATPase is scanty so far. Recently, measurements of the circular dichroism resulting from $n \rightarrow \pi^*$ and $\pi \rightarrow \pi^*$ transitions of the peptide backbone have been described [25–27]. While such studies in principle can yield information on the presence of α-helical, β, and random-coil structures in the protein, the interpretation of circular-dichroism spectra of Na^+/K^+-ATPase preparations is difficult due to scattering and absorption-flattening effects [25,27]. Chetverin, Brazhnikov and co-workers have carried out infrared spectroscopic studies of suspensions of particulate Na^+/K^+-ATPase in D_2O [28–30]. From a line-shape analysis of the amide I band, they estimated that about 22% of the peptide bonds are involved in α-helices and 22% in β-pleated sheets [30]. Experiments in which energy transfer between chromophores has been measured provided information on distances between inhibitor and substrate binding sites [31,32]. Distances between ion and substrate binding sites have been inferred from EPR and NMR experiments using magnetic probes such as Mn^{+2}, $^{205}Tl^+$ or ^{31}P [35–40].

In the following we describe a method by which the polarized infrared absorption of oriented layers of

Correspondence: H.-J. Apell, Department of Biology, University of Konstanz, D-7750 Konstanz, F.R.G.

Na^+/K^+-ATPase can be studied. By dodecylsulfate extraction of kidney microsomes [41] flat membrane fragments 0.2–1 μm in diameter containing oriented Na^+/K^+-ATPase molecules with a density of several thousand per μm^2 may be prepared [20–24]. Infrared spectra of these membrane fragments can be measured using the technique of attenuated total reflection (ATR) spectroscopy [42,43]. For this purpose a thin germanium plate is covered with a lipid bilayer with the polar groups of the outer phospholipid monolayer facing the aqueous medium into which the germanium plate is immersed (Figs. 1 and 2) [44]. Addition of a suspension of Na^+/K^+-ATPase membrane fragments to the medium leads to binding of fragments to the lipid bilayer. Binding is found to be virtually irreversible, the density of bound protein corresponding approximately one third of a monolayer of membrane fragments. Similar observations have been made previously in experiments with 'black' lipid films in which adsorption of Na^+/K^+-ATPase membrane fragments to the film has been detected by monitoring electrical signals associated with pump activity [45,46].

The ATR technique has several advantages compared to conventional infrared experiments. ATR measurements of aqueous systems are less impeded by water absorption than transmission experiments. Furthermore, the sensitivity is considerably increased by multiple reflexion of the infrared beam. The chief advantage of the ATR method consists in the possibility of obtaining polarized infrared spectra of oriented samples (Fig. 1). ATR studies have been performed in the last years with oriented lipid layers [47–54], proteins [55–59] and mixed lipid/peptide systems [60–63].

Most of these experiments have been performed with dry or hydrated multilayer samples. The application of ATR spectroscopy to biological samples, however, offers the possibility of in situ studies, e.g. structure-activity investigations with immobilized enzymes [64–66], as well as studies of drug-membrane interaction [44,67], protein adsorption to polymer surfaces [68,69], and cell growth [70]. In this paper in situ experiments are reported with immobilized membrane fragments containing Na^+/K^+-ATPase.

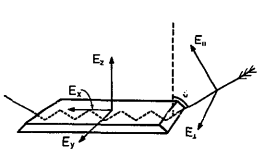

Fig. 1. Set-up for attenuated total reflection (ATR) spectroscopy. At an angle of incidence of $\vartheta = 45°$, total reflection of the infrared beam occurs in the germanium plate (50×20×1.25 mm). The electromagnetic field penetrates into the optically rarer medium beyond the reflecting interface over a distance of the order of the wavelength oi the radiation. This 'evanescent wave' is attenuated by absorption in the medium and in the lipid-protein layers (Fig. 2) covering the germanium surfaces. $E_\parallel$ and $E_\perp$ are the parallel and perpendicular polarized components of the electric field of the incident beam. E_x, E_y and E_z are the field components with respect to the coordinate system corresponding to the reflection plate. If the incident radiation is parallel (perpendicular) polarized, the electric field in the rarer medium is xy-(y)-polarized.

Materials and Methods

Materials

Phosphatidic acid (PA) and phosphatidylcholine (POPC) were obtained from R. Berchtold, Biochemical Laboratory, Bern, and sodium dodecylsulfate (SDS) from Pierce Chemical Co., Rockford,IL. Phospho*enol*-pyruvate, pyruvate kinase, lactate dehydrogenase, NADH and ATP (disodium salt, Sonderqualität) were from Boehringer, Mannheim. Deuterium chloride was from Aldrich-Chemie, Steinheim. All buffer salts were dissolved in D_2O and dehydrated twice under vacuum to remove residual H_2O. The pH was adjusted with deuterium chloride solutions in D_2O. 150 mM NaCl, KCl and Tris-DCl buffers were prepared by dissolving appropriate amounts of dehydrated salts in a stock buffer containing 1 mM EDTA, 30 mM imidazole and 5 mM $MgCl_2$, pD 7.5. All other reagents were analytical grade.

Enzyme preparation

Na^+/K^+-ATPase was prepared from the outer medulla of rabbit kidneys using procedure C of Jørgensen [41]. This method yields purified enzyme in the form of membrane fragments containing about 0.6 mg phospholipid and 0.2 mg cholesterol per mg protein [5,41]. The specific ATPase activity was determined by the pyruvate kinase/lactate dehydrogenase assay [71] and the protein concentration by the method of Lowry et al. [72] using bovine serum albumin as a standard. For most preparations the specific activity was in the range between 1500 and 2200 μmol P_i per h and mg protein at 37°C, corresponding to a turnover rate of 120–170 s^{-1} (based on a molar mass of 280000 g/mol). The suspension of Na^+/K^+-ATPase-rich membrane fragments (about 3 mg protein per ml) in buffer (25 mM imidazole, pD 7.5, 1 mM EDTA, 10 mg/ml saccharose) was frozen in samples of 100 μl; in this form the preparation could be stored for several months at −70°C without significant loss of activity.

1 mg membrane fragments were spun down in a Beckman Airfuge and resuspended in a buffer containing 20 mM imidazole, 1 mM EDTA, 1% saccharose, pH 7.5, in D_2O. This procedure was repeated twice to remove H_2O from the membrane fragments. The final pellet was resuspended in 200 μl Tris-DCl buffer to yield a 5 mg/ml suspension of fragments. Transport

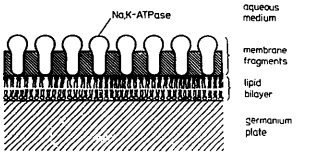

Fig. 2. Internal-reflection plate covered with lipid and protein layers. The germanium surface is initially coated with a phospholipid bilayer and is in contact with aqueous solution. The aqueous solution is replaced by a suspension of flat membrane fragments 0.2–1 μm in diameter containing oriented Na^+/K^+-ATPase molecules with a density of several thousand per μm^2. This leads to binding of membrane fragments to the lipid bilayer. The ATPase molecules are depicted with their cytoplasmic portions facing the aqueous medium, but the actual orientation of the membrane fragments is not known. Both the upper and the lower surface of the reflection plate (Fig. 1) are covered with lipid and protein.

activity of Na^+/K^+-ATPase in D_2O buffer was tested and showed no significant differences compared to measurements in H_2O.

Sample preparation

Supporting bilayer. The supporting bilayer membrane (Fig. 2) which has a function corresponding to a black lipid membrane [45,46] was prepared in two steps [44]. First a monolayer of dipalmitoylphosphatidic acid (DPPA) was transferred at 30 mN/m from the air/water interface of a LAUDA film balance (LAUDA, Königshofen, F.R.G.) to both sides of a germanium ATR plate by means of the Langmuir-Blodgett technique [73]. The subphase was a 10^{-4} M aqueous solution of $CaCl_2$. The DPPA-coated ATR plate was then mounted in a liquid sample cell, where it remained during the experiment. The bilayer was completed by adsorption of a POPC monolayer to the hydrophobic surface of the DPPA monolayer [44]. This step was achieved by filling the ATR cell with a solution containing POPC vesicles (1 mg/ml) 100 mM NaCl, 10^{-4} M $CaCl_2$ and 20 mM phosphate buffer pH 7. The adsorption process was monitored in situ. The bilayer was completed after about 30 min and was stable as long as it remained in contact with an aqueous medium.

Adsorption of membrane fragments. Membrane fragments were suspended in Tris-DCl buffer as described above, and the ATR cell was filled with the suspension. The time course of the adsorption of membrane fragments to the germanium plate was monitored in situ. Fig. 3A represents a sequence of IR-ATR spectra obtained with parallel polarized incident light from a typical adsorption process which reached equilibrium after 45 to 60 min. After this time the suspension of membrane fragments was replaced by pure buffer solution. Fig. 3B presents the results of a quantitative analysis of Fig. 3A. The sample remained absolutely stable with respect to the protein content during the whole experimental period of two days. However, some lipid loss occurred upon draining and refilling the cell with aqueous solutions.

ATR experiments and data analysis

Spectroscopic equipment. Spectra were scanned in single beam mode using a BRUKER IFS 45 FT-IR spectrometer equipped with a DTGS detector and a special ATR attachment with cylindrical mirrors for optimum beam-handling. The spectral resolution was 2 cm^{-1} with a zero filling factor of 2 leading to a point distance of 1 cm^{-1}. The ATR plate ($52 \times 20 \times 1.25$ mm^2) was trapezoid with an angle of incidence of $\theta = 45 \pm 2.5°$. Collimation occurred only in the horizontal plane whereas a parallel beam was used in the vertical plane. This principle resulted in a better control of the number R of active internal reflections and of the angle of incidence θ than is generally achieved by commercial ATR attachments. Both R and θ have a significant meaning for the quantitative analysis of the spectra. The length of the immobilized membrane was 38 mm on both sides of the plate, thus resulting in $R = 30$ active internal reflections. This number is optimal for monolayer and submonolayer spectroscopy in aqueous environment, since the small quantity of substance in a monolayer requires a large number of reflections, whereas a small number of reflections would be better for the compensation of the strong solvent (D_2O, H_2O) absorption bands. The ATR cell was thermostatted to $25 \pm 0.5°C$.

Data handling. Spectra were smoothed with a smoothing factor that did not reduce the peak height of the CH-stretching bands of the lipid. Absorbance difference spectra (except dichroic difference spectra) are all calculated with scaling factors of 1, i.e. they represent the correct ('hardware') difference between sample (membrane fragments) and reference (supporting bilayer); compare Fig. 2. On the other hand, dichroic difference spectra ($A^*(\bar{\nu})$) are weighted difference spectra between the parallel polarized ($A_\parallel(\bar{\nu})$) and perpendicular polarized ($A_\perp(\bar{\nu})$) spectra of the same sample [59]:

$$A^*(\bar{\nu}) = A_\parallel(\bar{\nu}) - R_{ISO} \cdot A_\perp(\bar{\nu}) \quad (1)$$

where R_{ISO} denotes the dichroic ratio of an isotropic sample which is generally different from unity in ATR spectroscopy [42,51,59,67]. $A_\parallel(\bar{\nu})$ and $A_\perp(\bar{\nu})$ denote the decadic absorbance spectra with parallel and perpendicular polarized incident light, respectively. Obviously, in the dichroic difference spectrum $A^*(\bar{\nu})$ all absorption bands resulting from isotropically oriented transition dipole moments [42] are eliminated. Solving

Eqn. 1 for the parallel-polarized contribution from the oriented part of the sample results in

$$A_{\parallel}^{\mathrm{ori}}(\tilde{\nu}) = \frac{R_{\mathrm{ori}}}{R_{\mathrm{ori}} - R_{\mathrm{iso}}} A^{*}(\tilde{\nu}) \qquad (2)$$

where $R_{\mathrm{ori}} = A_{\parallel}^{\mathrm{ori}}(\tilde{\nu})/A_{\perp}^{\mathrm{ori}}(\tilde{\nu})$ denotes the mean dichroic ratio of the oriented part of the sample at wavelength $\tilde{\nu}$. Eqn. 2 gives access to a quantitative analysis of the polarized part of a complex spectrum, provided reliable information on R_{iso} and R_{ori} is available. In this paper dichroic difference spectra according to Eqn. 1 are presented from membrane fragments in contact with Tris-, K^+- and Na^+-buffer. Eqn. 2 was used in an approximate way.

Quantitative analysis. Determination of surface concentrations was performed in the same way as described in Ref. 74, using the following optical constants: For germanium (ATR plate) a wavelength-independent refractive index of $n_1 = 4.0$ was used. Local refractive indices of the protein were estimated from experiments with lysozyme mono- and multilayers (to be published). The wavelength-dependent refractive indices of liquid D_2O were approximated from those of liquid H_2O [75] taking the isotope shift into account. The integrated molar absorption coefficients of protein bands are based on the value for the amide I band as determined with alamethicin [61]. The values for ν(NH), ν(CH) and amide II were determined with lysozyme. Finally the values of $\nu_{as}(COO^-)$ and $\nu_s(COO^-)$ are rough approximations obtained from sodium polyglutamate and sodium acetate. For ν(CH) of lipid hydrocarbon chains a refractive index $n_2 = 1.50$ was assumed and the integrated molar absorption coefficient of the whole ν(CH) complex was determined from Langmuir-Blodgett monolayers. The optical constants are summarized in Table I.

To introduce the imaginary part of the refractive index, some basic work must be done for the refinement of the optical parameters. The electrical field components (cf. Fig. 1) were calculated with the thin-layer approximation [42,43] which is applicable since the maximum film thickness (cf. Fig. 2) is expected to be 11–13 nm, which is small in comparison to the penetration depth of 0.19 μm (ν(NH)) to 0.45 μm ($\nu_s(COO^-)$).

TABLE I

Optical parameters used for quantitative data analysis

Absorption band	Wavenumber (cm^{-1})	$\int \epsilon(\tilde{\nu}) d\tilde{\nu}$ [1] (cm/mol)	n_2 [2]	n_3 [3]
ν(NH)	≈ 3300	$2.09 \cdot 10^7$	1.40	1.27
ν(CH) protein	2800–3000	$6.60 \cdot 10^5$	1.47	1.20
ν(CH) lipid	2800–3000	$1.32 \cdot 10^8$	1.50	1.20
Amide I	≈ 1650	$2.74 \cdot 10^7$	1.40	1.32
Amide II	≈ 1540	$8.25 \cdot 10^6$	1.40	1.31
$\nu_{as}(COO^-)$	≈ 1580	≈ $6.1 \cdot 10^7$	1.37	1.31
$\nu_s(COO^-)$	≈ 1400	≈ $2.3 \cdot 10^7$	1.37	1.29

[1] Integrated decadic molar absorption coefficient, $\epsilon = A/(cd) = -\log T/(cd)$.
[2] Local refractive index of sample.
[3] Approximate refractive index of liquid D_2O.

Background spectra

To eliminate the contributions of the aqueous phase, background spectra were measured before adsorption of Na^+/K^+-ATPase membranes. The cell with the PA/POPC-coated germanium plate was filled with 150 mM potassium-buffer and the infrared spectra were recorded under parallel and perpendicular polarisation. Each measurement consisted of an average of 2560 single spectra in parallel polarisation and 3072 single spectra in perpendicular polarisation in the wavenumber range between 4000 and 600 cm^{-1}. The potassium-buffer was assumed to produce the same spectrum as the Na^+ buffer does, since all the other components were identical. After flushing with 5 ml 150 mM Tris-DCl buffer, the measurement was repeated and the results were stored in the computer memory for further use.

Stability of membrane assembly

Lipid. $3.9 \cdot 10^{-11}$ mol/cm^2 POPC which is about 12% of the outer monolayer of the supporting membrane (Fig. 2) was lost from the ATR plate upon buffer exchange from K^+ to Tris. This results in a corresponding overcompensation of POPC in the spectra in K^+ and Na^+ environment, as seen from the C=O stretching band of the fatty acid ester (≈ 1730 cm^{-1}) (Fig. 5) and in the CH stretching region (Fig. 6). A further loss of lipid, predominantly of POPC, of about $3.2 \cdot 10^{-11}$ mol/cm^2 (≈ 10% of the POPC monolayer) was observed when the buffer in contact with the adsorbed membrane fragment was changed from $Tris^+$ to K^+. The final K^+-Na^+ buffer exchange resulted in an additional loss of $2.0 \cdot 10^{-11}$ mol/cm^2, (≈ 6% of the POPC monolayer). The overall phospholipid loss was therefore 28% of a POPC monolayer (assumed area per molecule: 50 $Å^2$). It should be noted that no significant lipid loss was observed, when the aqueous phase was exchanged for a solution of identical composition.

Protein. The calculated protein surface concentrations of membrane fragments in Tris, K^+ and Na^+ buffer differed by less than 1%. That means that Na^+/K^+-ATPase binds tightly to the supporting bilayer and that lipid loss probably results from uncoated parts of this layer (see Discussion).

Results

Adsorption kinetics

At the beginning of the experiment, the drained cell was filled with 2 ml Tris-DCl buffer containing 500 μg

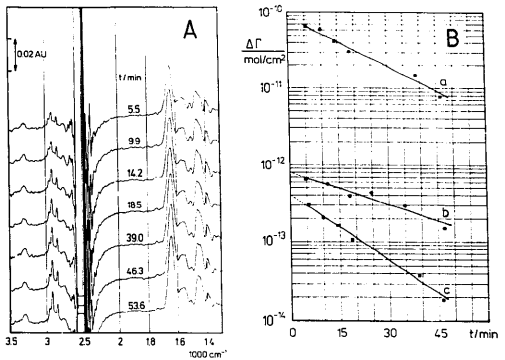

Fig. 3. Adsorption kinetics of membrane fragments to a germanium ATR plate coated with a phospholipid bilayer (Fig. 2). (A) Sequence of parallel polarized spectra scanned in the time range 5 to 50 min. (B) Semi-logarithmic plot of difference surface concentrations $\Delta\Gamma(t) = \Gamma(53.6\ \text{min}) - \Gamma(t)$ vs. time t. Lipid surface concentration was determined from the integrated absorbance of the whole ν(CH) band complex (3000–2800 cm^{-1}) and normalized to a mean cross-section of 50 $Å^2$/molecule (curve a) which is typical for POPC. Protein surface concentrations were calculated from the integrated absorbances of amide I, I′ in D_2O(l) medium (curve c) and of amide II in H_2O(l) medium (curve b). Only the slow part of fragment adsorption is shown in the figure. A considerable fraction of membrane fragments adsorbs fast (probably diffusion-controlled) within $0 < t < 5$ min (see text). The final surface fractions are $x_P = 0.12$ for the protein and $x_L = 0.22$ for the lipid (normalized to POPC).

membrane fragments. To record the time course of adsorption, measurements in parallel polarisation were taken in sequences of 128 single spectra. A typical sequence is presented in Fig. 3A. The adsorption process is terminated after about 50 minutes. In order to eliminate background absorption (dissolved fragments, etc.) the difference spectra between equilibrium ($t = 53.6$ min) and time t (cf. Fig. 3A) were used for kinetic analysis. Fig. 3B presents a semi-logarithmic plot of the surface concentration difference, $\Delta\Gamma = \Gamma(53.6\ \text{min}) - \Gamma(t)$ as a function of time t for the total ν(CH) complex (≈ 2900 cm^{-1}, curve a) and the amide I, I′ band (≈ 1650 cm^{-1}, curve c). The time-dependent increase of the amide II band (≈ 1550 cm^{-1}, curve b) is taken from an experiment in H_2O environment (cf. Table I). The relatively good linear fit points to an approximate first

TABLE II

Results of a linear regression of the form $\ln \Delta\Gamma = -kt + \ln \Delta\Gamma_0$, *taken from a semi-logarithmic plot of difference surface concentrations of lipids and protein (Fig. 3b)*

The error limits of R and $\Delta\Gamma_0$ correspond to a 95% confidence interval.

Band	k (min^{-1})	$t_{1/2}$ [1] (min)	$\Delta\Gamma_0$ [2] (mol/cm^2)	Γ_f [3] (mol/cm^2)	$\Gamma_f - \Delta\Gamma_0$ [4] (mol/cm^2)
ν(CH) lipid [5]	0.0505 ± 0.0079	13.7	$(8.98 \pm 0.19) \cdot 10^{-11}$	$1.45 \cdot 10^{-10}$	$5.52 \cdot 10^{-11}$
Amide I, I′ [6]	0.0649 ± 0.0067	10.7	$(4.02 \pm 0.80) \cdot 10^{-13}$	$9.09 \cdot 10^{-13}$	$5.07 \cdot 10^{-13}$
Amide II [7]	0.0334 ± 0.0097	20.8	$(8.13 \pm 2.15) \cdot 10^{-13}$	$1.16 \cdot 10^{-12}$	$3.50 \cdot 10^{-13}$

[1] Half-time: $t_{1/2} = (\ln 2)/k$.
[2] Difference surface concentration at $t = 0$, linear extrapolation (see text).
[3] Final surface concentration in Tris buffer.
[4] Amount of membrane fragments that adsorbed in time ≪ 5 min.
[5] Total CH-stretching band (cf. Table I). The contribution from the protein was subtracted, assuming 8130 CH bonds per Na^+/K^+-ATPase molecule. The lipid matrix was normalized to POPC (50 $Å^2$/molecule) Tris-DCl, pD 7.5, according to Fig. 3B (curve a).
[6] Protein, normalized to Na^+/K^+-ATPase (1318 amino acids per $\alpha\beta$-subunit), Tris-DCl, pD 7.5, according to Fig. 3B (curve c).
[7] Partly overlapped by $\nu_{as}(COO^-)$. Integration interval: 1585–1500 cm^{-1}. Protein was normalized to Na^+/K^+-ATPase (1318 amino acids per $\alpha\beta$-subunit). Tris-HCl, pH 7.5, according to Fig. 3B (curve b).

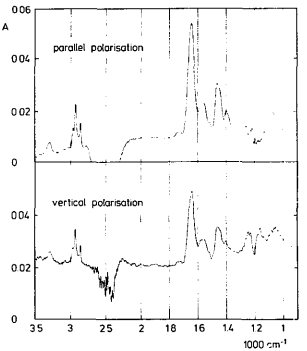

Fig. 4. Polarized IR-ATR overview spectra of adsorbed membrane fragments with Na^+/K^+-ATPase in the spectral range 3500–900 cm^{-1}. Surface coverage by protein and by lipid of membrane fragments is about 12%, and 22%, respectively, of the POPC supporting membrane. The aqueous environment consisted of 150 mM Tris-DCl, pD 7.5, 5 mM $MgCl_2$, 1 mM EDTA and 30 mM imidazole in D_2O at 20 °C. The angle of incidence was $\vartheta = 45°$ and number of active internal reflections was $R = 30$. The supporting phospholipid bilayer (cf. Fig. 2) in the same aqueous environment was subtracted with scaling factors unity. Spectra were smoothed under conditions which did not reduce the peak height of ν(CH) bands.

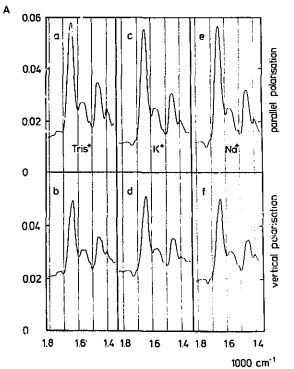

Fig. 5. Polarized IR-ATR spectra of adsorbed membrane fragments with Na^+/K^+-ATPase in the spectral range 1800–1400 cm^{-1}. The aqueous (D_2O) medium was changed from 150 mM Tris-DCl (a, b) via 150 mM KCl (c, d) to 150 mM NaCl (e, f), pD 7.5, $T = 20$ °C. The other conditions are described in the legend to Fig. 4. All scaling factors were unity.

order process at least between $t \approx 5$ minutes and equilibrium. The results of a linear regression of the form $\ln \Delta\Gamma = -kt + \ln \Delta\Gamma_0$ are summarized in Table II.

Polarized IR-ATR spectra in Tris, K^+ and Na^+ media

Fig. 4 shows polarized survey spectra of Na^+/K^+-ATPase in adsorbed membrane fragments in the 3500–900 cm^{-1} range. The surrounding aqueous medium was Tris-DCl buffer, pD 7.5. Under this condition, the Na^+/K^+-ATPase may be assumed to be predominantly in E_1 confirmation [76,77]. A DPPA/POPC bilayer in contact with the same medium served as reference. Scaling factors for sample and reference spectra were unity. In the regions of strong liquid D_2O absorption ($\nu(D_2O)$, ≈ 2500 cm^{-1}; $\delta(D_2O)$, ≈ 1200 cm^{-1}) there is a slight solvent overcompensation which results from the reduced effective thickness of the aqueous medium due to membrane fragment adsorption. Prominent protein absorption bands are [78]: ν(NH), NH-stretching at ≈ 3300 cm^{-1} which reflects the hard core of the protein [28–30]; amide I, I′ ($\approx 80\%$ C=O-stretching of amide group, the apostrophe denoting the vibration of the *N*-deuterated group) at ≈ 1645 cm^{-1}; $\nu_{as}(COO^-)$ (antisymmetric CO_2^- stretching of gluta-

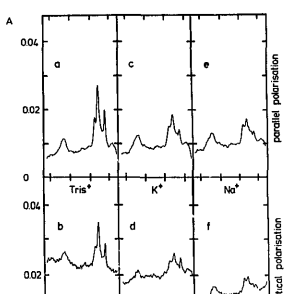

Fig. 6. Polarized IR-ATR spectra of adsorbed membrane fragments with Na^+/K^+-ATPase in the spectral range 3500–2700 cm^{-1}. The aqueous (D_2O) medium was changed from 150 mM Tris-DCl (a, b) via 150 mM KCl (c, d) to 150 mM NaCl (e, f), pD 7.5, $T = 20$ °C. The significant reduction of ν(CH) band intensities results predominantly from POPC loss from the supporting bilayer, see text. The other conditions are described in the legend to Fig. 4. All scaling factors were unity.

mate, aspartate) at ≈ 1580 cm^{-1}; amide II (≈ 60% NH-bending) at ≈ 1540 cm^{-1}; amide II′ (partly ND-bending) at ≈ 1460 cm^{-1}; $\nu_s(COO^-)$ (symmetric CO_2^- stretching of glutamate and aspartate) at ≈ 1400 cm^{-1}.

The most intense bands of the lipid matrix are: ν(CH) (CH-stretching) at 2800–3000 cm^{-1} and ν(C=O) (C=O-stretching of fatty acid ester) at ≈ 1730 cm^{-1}. The band near 1070 cm^{-1} might predominantly result from the carbohydrate part of the β subunit. Fig. 5 and 6 present those sections of the spectra of Na^+/K^+-ATPase in Tris, K^+ and Na^+ environment which are discussed in this paper. The basic data for quantitative analysis and the results are summarized in Table III. The most significant results will be discussed in the following.

Surface coverage

The mean surface concentration of α, β-units of Na^+/K^+-ATPase is found to be $\Gamma_P = 9.09 \cdot 10^{-13}$ mol/cm^2. There is no loss of protein during the change of medium (Tris → K^+ → Na^+) in contrast to the behaviour of the lipids. As already mentioned in Materials and Methods, a first POPC loss of $3.9 \cdot 10^{-11}$ mol/cm^2 was observed during the measurement of the spectra of the supporting bilayer which served as reference. This amount is still included in the surface concentrations of lipids in K^+ and Na^+ environment indicated in Table III. The original lipid surface concentration resulting from the membrane fragments is found to be $\Gamma_{LT} = 1.45 \cdot 10^{-10}$ mol/cm^2 in Tris-DCl buffer. This value is normalized to POPC. Assuming an area per molecule of 50

TABLE III

Basic spectroscopic data and results of quantitative analysis of the spectra of adsorbed membrane fragments with Na^+/K^+-ATPase in Tris-DCl, K^+ and Na^+ environment, pD 7.5, 20°C

Absorption band		$\bar{\nu}$ (cm^{-1})	$\int A_\parallel d\bar{\nu}$ (cm/mol)	$\int A_\perp d\bar{\nu}$ (cm/mol)	R [1]	θ [2] (deg)	Γ (mol/cm^2)	N [3]	Note
Protein									
ν(NH)	Tris	3285	0.315	0.197	1.6	65–50	$2.59 \cdot 10^{-10}$	329	
	K^+	3285	0.330	0.138	2.4	46–24	$2.84 \cdot 10^{-10}$	313	4
	Na^+	3285	0.319	0.161	2.0	52–35	$2.86 \cdot 10^{-10}$	315	
ν(CH)		3000–2800	0.293	0.212	1.38	55	$7.38 \cdot 10^{-9}$	8130	5
Amide I, I′	Tris	1645	1.828	1.117	1.64	60–57	$9.101 \cdot 10^{-13}$	1317	
	K^+	1645	1.819	1.117	1.63	60–57	$9.079 \cdot 10^{-13}$	1317	6
	Na^+	1645	1.824	1.118	1.63	60–57	$9.095 \cdot 10^{-13}$	1317	
$\nu_s(COO^-)$	Tris	1397 (∥) 1403 (⊥)	0.125	0.034	3.7	0–37	$8.0 \cdot 10^{-11}$	88	
	K^+	1398 (∥) 1400 1383 (⊥)	0.079	0.029	2.7	30–43	$5.4 \cdot 10^{-11}$	60	7
	Na^+	1399 (∥) 1403 (⊥)	0.069	0.053	1.3	90–66	$6.0 \cdot 10^{-11}$	66	
Lipids									
ν(CH)	Tris	3000–2800	0.851	0.530	1.60	25–43	$1.45 \cdot 10^{-10}$	1 [10]	
	K^+	3000–2800	0.435	0.246	1.77	0–34	$7.39 \cdot 10^{-11}$	1	8
	Na^+	3000–2800	0.314	0.172	1.83	0–34	$5.43 \cdot 10^{-11}$	1	
ν(C=O)	Tris	1735	0.034	0.042	0.81	90	$2.4 \cdot 10^{-11}$	1 [10]	
	K^+	1735	−0.046	−0.063	0.73	90	$-3.4 \cdot 10^{-11}$	1	9
	Na^+	–	–	–	–	–	–	–	

[1] R is defined to be $\int A_\parallel d\bar{\nu} / \int A_\perp d\bar{\nu}$.

[2] Mean angle between transition dipole moment and z-axis (see also Ref. 42). Protein: Minimum order parameter determined from $\nu_s(COO^-)$ is $S = 0.4$ Assumption for protein: $0.4 \leq S \leq 0.8$. Lipids: Minimum order parameter of $S = 0.2$. Assumption for lipids: $0.2 \leq S \leq 0.5$, cf. Discussion.

[3] Number of corresponding functional groups per Na^+/K^+-ATPase molecule.

[4] Mean of protonated NH groups is 319 i.e. 24% of amide groups are not accessible by D_2O. Integration interval: 3400–3200 cm^{-1}.

[5] Calculated integrated decadic absorbances. Isotropic orientation assumed. Integration interval: 3000–2800 cm^{-1}.

[6] Mean protein surface concentration is $\bar{\Gamma} = 9.09 \cdot 10^{-13}$ mol/cm^2. Integration interval: 1704–1596 cm^{-1}.

[7] 117 Asp and Glu residues per α/β unit [11]. Note the significant orientational changes during a Tris-K^+-Na^+ transition. Integration interval: 1415–1360 cm^{-1}.

[8] Effective lipid band. Protein contribution subtracted. Surface concentration normalized to POPC. For discussion of lipid loss cf. Materials and Methods. Integration interval: 3000–2800 cm^{-1}.

[9] Surface concentration normalized to POPC. Note discrepancy with respect to ν(CH). For discussion of lipid loss cf. Materials and Methods. Integration interval: 1760–1700 cm^{-1}.

[10] Normalized to POPC.

$Å^2$ one obtains a lipid surface fraction of $x_{LT} = 0.22$ if the lipids are arranged in a bilayer. The protein surface fraction may be calculated by means of the molecular cross section (projection to the membrane plane) of 2132 $Å^2$ as determined by image reconstruction from electron micrographs [79]. It results in $x_P = 0.12$. Thus the surface fraction of membrane fragments in Tris-DCl buffer is found to be $x_{MT} = x_{LT} + x_P = 0.34$, i.e., one-third of the supporting bilayer is covered by membrane fragments.

Exchanging Tris buffer by K^+ buffer resulted in an additional lipid loss of $3.2 \cdot 10^{-11}$ mol/cm^2 most probably from the POPC monolayer of the supporting membrane (see Discussion). Finally further $2.0 \cdot 10^{-11}$ mol/cm^2 lipids (POPC) was lost upon buffer change from K^+ to Na^+. This process is paralleled by the formation of a negative C=O-stretching band at 1735 cm^{-1}, a fact which needs further discussion.

Non-exchangeable amide protons

Na^+/K^+-ATPase contains 24% of amide groups which are not accessible for liquid D_2O within a time range of several days. H^+/D^+ exchange is not affected by a change of the medium from Tris via K^+ to Na^+ (cf. Fig. 6 and Table III).

Orientation of transition moments

Amide I, I′. This most significant band for secondary structure determination by IR spectroscopy [78] exhibits a slight mean polarization towards the membrane plane. The measured dichroic ratio is 1.64 (cf. Table III) whereas the expected ratio for isotropic amide groups is $R_{iso} = 1.77$. Changes upon buffer exchange could only be detected by dichroic difference spectra (see below).

ν(NH). There is evidence for a slight reorientation of NH bonds of non-exchangeable amide protons during buffer exchange from Tris to K^+ and Na^+. In Tris environment the mean direction of NH bonds is expected to form an angle of 50° to 65° with respect to the *z*-axis. In K^+ and Na^+ the corresponding angle is found to be 24° to 52° (cf. Table III). Since in the latter case there is a significant deviation from isotropy, one may conclude that the hard (non-exchanging) core of the protein contains ordered segments which are partly reoriented by buffer exchange. Corresponding effects are observed with dichroic difference spectra (Fig. 7B) in the amide I, I′ and amide II region (see below).

$\nu_s(COO^-)$. Significant orientation changes upon buffer exchange are observed with the carboxylate groups of Asp and Glu. In Tris-DCl buffer the mean orientation of the bisectors of the angle of OCO is predominantly towards the *z*-axis (normal to the membrane). In K^+ buffer it assumes an intermediate direction and in Na^+ buffer it is inclined predominantly toward the membrane surface.

ν(CH). CH-stretching vibrations of the protein are assumed to have an isotropic distribution. The calculated integrated absorbances are indicated in Table III. Subtraction of these values from the overall integral absorbances results in the contribution of the lipids in the membrane fragments. It is seen from Table III that the dichroic ratio of the entire ν(CH) complex increases from 1.60 to 1.83 upon exchange of the buffers (Tris → $K^+ \rightarrow Na^+$). On the other hand all these values are unusually high, since for a flat oriented bilayer on the ATR plate (cf. Fig. 2) one would expect an overall dichroic ratio of ν(CH) below the isotropic value of $R_{iso} = 1.38$. This fact is not understood at present.

ν(C=O). The mean orientation of the C=O double bonds of the fatty acid ester groups is found to be parallel to the membrane plane (Table III). The polarization of ν(C=O) is consistent with a lamellar, liquid-crystalline ultrastructure in contrast to the overall polarization of ν(CH), see above. Furthermore, it should be noted that the intensity of ν(C=O) is about 6-times too small for a phospholipid, since the peak absorbances of ν(C=O) and $\nu_s(CH_2)$ should be approximately equal as shown, e.g., by the IR ATR spectrum of the POPC monolayer of the supporting bilayer under similar conditions [44].

Dichroic difference spectra $A^*(\tilde{\nu})$

A complementary way to analyse polarized spectra is the use of dichroic difference spectra as introduced by Eqn. 1. The main problem arising is to get reliable information on the isotropic dichroic ratio $R_{iso} = (E_z^2 + E_x^2)/E_y^2$, which depends on the optical constants of ATR crystal, sample and rarer medium (aqueous solution). Both, refractive index *n* and absorption index *k* depend on the wavenumber $\tilde{\nu}$. However, only approximate information on local refractive indices of the sample and on the complex refractive index of D_2O is available so far. In this analysis the absorption index *k* was neglected (cf. Discussion). Local refractive indices for protein groups were estimated from thin lysozyme layers (to be published) and the corresponding refractive index of the D_2O environment was approximated from H_2O data [75]. It follows that R_{iso} varies from 1.4 for ν(CH) to 1.9 for $\nu_{as}(COO^-)$. Values of 1.77, 1.73 and 1.71 were obtained for amide I, I′, amide II and amide II′, respectively. In order to demonstrate the importance of the parameter R_{iso}, $A^*(\tilde{\nu})$ spectra of Na^+/K^+-ATPase membrane fragments in Tris-DCl (cf. Fig. 4) were plotted in Fig. 7A with $R_{iso} = 1.4$, 1.6, 1.8 and 2.0. Fig. 7B presents $A^*(\tilde{\nu})$ spectra with $R_{iso} = 1.77$ (typical for amide I, I′) for Na^+/K^+-ATPase membrane fragments in Tris, K^+ and Na^+ environment, respectively.

Figs. 7A, B may be interpreted in the following way. In principle a positive band in the $A^*(\tilde{\nu})$ spectrum points to corresponding transition moments directed

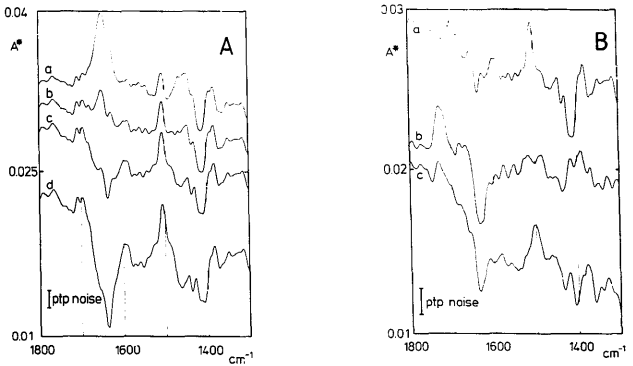

Fig. 7. IR-ATR dichroic difference spectra $A^*(\bar{\nu}) = A_{\parallel}(\bar{\nu}) - R_{iso} \cdot A_{\perp}(\bar{\nu})$ (see text) of adsorbed membrane fragments with Na^+/K^+-ATPase in the spectral range 1800–1300 cm^{-1}. A^* bands exceeding the peak-to-peak noise level of $1.6 \cdot 10^{-3}$ decadic absorbance units reflect ordered parts in the fragments. Positive signals indicate predominant orientation of corresponding transition moments towards the z-axis (normal to the membrane, Figs. 1 and 2), negative bands indicate predominant orientation towards the xy-plane (plane of the membrane). (A) The importance of the dichroic ratio of an isotropic sample R_{iso} (see text) is demonstrated by calculating A^* spectra from the polarized IR-ATR spectra of membrane fragments in Tris environment (cf. Fig. 4), with $R_{iso} = 1.4$ (a), 1.6 (b), 1.8 (c) and 2.0 (d), respectively. For the amide I, I′ band at ≈ 1650 cm^{-1}, $R_{iso} \approx 1.77$ is calculated. The relative invariance of some bands results from a distinct z-($\parallel$-)orientation (≈ 1506 cm^{-1}) or xy-($\perp$-)orientation (≈ 1410 cm^{-1}). (B) Dichroic difference spectra with $R_{iso} = 1.77$. Membrane fragments in 150 mM Tris-DCl (a), 150 mM KCl (b) and 150 mM NaCl (c). Significant spectral changes occur in the amide I, I′ region, near 1500 cm^{-1} and near 1400 cm^{-1}. General conditions see Fig. 4.

predominantly towards to z-axis, whereas a negative band points to a predominant direction towards to xy-plane (plane of the membrane, cf. Figs. 1, 2). The main result of Fig. 7A is that accurate knowledge on R_{iso} is required in order to get relevant information from amide I, I′ (≈ 1650 cm^{-1}), amide II (≈ 1540 cm^{-1}) and amide II′ (≈ 1450 cm^{-1}). However, there are three bands that are much less affected by R_{iso}, namely two positive bands at 1506 cm^{-1} and ≈ 1385 cm^{-1}, and one negative band at ≈ 1412 cm^{-1}. According to Eqn. 1, such A^*-bands result from either distinctly parallel or perpendicular polarized bands, respectively. They indicate the presence of highly ordered parts in a complex system. Probably all three bands result from amino acid side chains, since correspondingly strong polarization effects are absent or randomized in the amide I, I′ region (Fig. 7B). There is no definite assignment available at present. For instance, the S-shaped band at 1400 cm^{-1} might result from two populations of -COO^- groups, one with the OCO-bisector predominantly parallel to xy-plane (1412 cm^{-1}) and the other with the bisectors aligned along the z-axis. Furthermore, the orientations of the groups associated with all three bands seem to be affected by a change of the medium from Tris-DCl via K^+ to Na^+.

Corresponding responses are also observed in the amide I, I′ and amide II′ regions. The following preliminary interpretation may be given for the data of Fig. 7B: The Tris-DCl to K^+ transition leads to a reorientation of amide groups with the C=O double bonds predominantly parallel to the plane of the membrane (xy-plane). The extent of reorientation may be estimated from Eqn. 2 by assuming the angle between the corresponding transition moments and the z-axis to be $\theta = 90°$. For $0.4 \leq S \leq 0.8$ (See Discussion, the order parameter S is a measure for the degree of fluctuation of a molecular segment. Limiting values are $S = 0$ for an isotropic phase and $S = 1$ for a crystalline phase.) the resulting range for the dichroic ratio of the reoriented sequence is $1.32 \geq R_{ori} \geq 1.00$ [42]. The integral over the amide I, I′ band of the A^* spectrum in K^+ environment (Fig. 7B, curve b) is found to be ≈ -0.1 cm^{-1}. The corresponding integrated absorbances for $\parallel$- and $\perp$-polarized incident light are then obtained from Eqn. 2 using $R_{iso} = 1.77$, resulting in a mean fractional surface concentration of $\Gamma_f \cong 1.2 \cdot 10^{-13}$ mol/cm^2 which indicates that about 13% of the amino acids undergo a conformational change upon Tris/K^+ buffer exchange. This change of secondary structure is paralleled by a depolarization of both, the 1506 cm^{-1} band and the

S-shaped band at 1400 cm^{-1}. The latter probably reflects a significant reorientation of $-COO^-$ groups of Asp and Glu upon buffer exchange. As reflected by spectra b and c in Fig. 7B, the original structure of Na^+/K^+-ATPase in Tris-DCl buffer is partly restored when replacing K^+ buffer by Na^+ buffer. For details on a quantitative analysis the reader is referred to reference [74].

Discussion

In this communication we have shown that IR-ATR spectroscopy enables quantitative in situ studies of membrane fragments with Na^+/K^+-ATPase under similar conditions as used in black film experiments [45,46]. This allows a comparison of kinetic data [45,46,80,81] with molecular structure. Some points of interest will be discussed in more detail below.

Adsorption kinetics, surface coverage and stability of membrane fragments

Two kinetic steps may be distinguished during adsorption, a fast, probably diffusion-controlled process, followed by a slower reaction which may be approximated by first-order kinetics. The initial step (spectroscopically not resolved) resulted in 30–60% of the final surface coverage whereas the slow step exhibited a half-time $t_{1/2}$ of 11 to 21 min, cf. Table II and Fig. 3. These findings are consistent with the kinetics of adsorption of membrane fragments to black lipid films, as determined from measurements of transient pump currents [46]. Considering the spectral range between 1300 and 1600 cm^{-1} in Fig. 3A, there is some evidence for a structural and/or compositional difference between fast ($t \leq 5.5$ min) and slowly ($t > 5.5$ min) adsorbed fragments. The surface coverage by protein calculated from the spectroscopic data presented above was $\Gamma_P = 9.09 \cdot 10^{-13}$ mol/cm^2, i.e., about 12% of the exposed POPC surface. The associated lipid matrix covered about 22%, thus the equilibrium surface coverage by membrane fragments in Tris-DCl buffer, pD 7.5 was found to be 34%. This value is a critical parameter for the analysis of transient pump currents [46,81]. From the spectral data presented here it is not possible, however, to distinguish between membrane fragments bound with the extracellular side and membrane fragments bound with the cytoplasmic side facing the lipid bilayer.

As already mentioned above, lipid surface coverage was calculated from the ν(CH) band taking POPC as a reference phospholipid (cross-section 50 $Å^2$ per molecule). Considering, however, the intensity of the ν(C=O) band of the fatty acid ester groups of phospholipids, one has to conclude that only a minor part of the ν(CH) intensity can result from phospholipids, because the lipid surface coverage as calculated from ν(C=O) is $\Gamma_{POPC}^{(C=O)} = 2.4 \cdot 10^{-11}$ mol/cm^2 which is 6-times less than the value calculated from the ν(CH) band. Very strong polar interactions (hydrogen bonding) between the ester carbonyl groups and the protein could result in band broadening, i.e. reduction of peak height. This explanation, however, is unlikely, since the molar lipid/protein ratio, $\Gamma_{POPC}^{(CH)}/\Gamma_P \equiv 160$, seems too high. A more realistic explanation is that 5/6 of the lipid matrix does not consist of phospholipids. In the applied method for fragment isolation (preparation C of Jørgensen [41]), sodium dodecylsulfate (SDS) incubation is an essential step. It might be that during this process phospholipid molecules are replaced by SDS. This uncertainty with respect to the lipid composition requires further experiments.

Adsorbed fragments are strongly bound, since no protein loss could be detected during a typical experimental period of two days. However, significant loss of POPC from probably uncovered regions of the supporting bilayer was noticed during buffer exchange. Draining of the cell is one reason for the loss. Electrolyte composition (especially Tris or K^+), however, could also have an influence. Experiments for elucidation are in progress.

Structural changes during Tris → K^+ → Na^+ buffer exchange

Secondary structural changes of the Na^+/K^+-ATPase as revealed by the amide I, I′ band are not easy to be detected by IR spectroscopy of a membrane fragment suspension [28–30] as well as by IR-ATR spectroscopy of adsorbed fragments (this paper). Although the ν(NH) band of the non exchanging core of the protein (about 24% of the amino acids) indicated a structural change upon buffer exchange, there is no evidence for such a conformational transition from the overall dichroic ratio of the amide I, I′ band (cf. Table III). Dichroic difference spectra, Figs. 7A and B, however, indicate that a conformational change may occur in the peptide backbone. The estimate of 13% of amino acids involved in the Tris → K^+ transition has to be considered as preliminary since the relevant optical parameters are only approximately known at present (Table I).

Further indications for possible structural changes of amino acid side chains is obtained from $\nu_s(COO^-)$ of Asp and Glu (cf. Table III and Fig. 7B), as well as from a so far not assigned band at 1506 cm^{-1} (Figs. 7A and B).

The determination of molecular orientation (cf. Table III) requires knowledge of the ultrastructure of membrane assembly [42] and of the local order parameters of functional groups. A layered, liquid-crystalline ultrastructure according to Fig. 2 was assumed. Electron microscopic investigations are in progress in order to get more information on the ultrastructure obtained under our conditions of sample preparation as well as on its stability during buffer exchange. There is good

evidence, that adsorbed fragments remain stable during the experimental period, see above.

The range of local order parameters was for lipids $0.2 \leq S \leq 0.5$ and for the protein $0.4 \leq S \leq 0.8$. The minimum values could be calculated from our data using the largest dichroic ratios of two reference bands (protein: $\nu_s(COO^-)$, Tris buffer, $R = 3.7$, $R_{iso} = 1.82$; lipids: $\nu(CH)$, Na^+ buffer, $R = 1.83$, $R_{iso} = 1.38$). If S_{min} would be smaller than 0.4 and 0.2, respectively, calculated dichroic ratios would be smaller than the corresponding experimental values for any angle θ, cf. Table III. The maximum values of order parameters were estimated. The range of S for lipids is consistent with NMR data [86].

Line shape analysis

Conventional line shape analysis [59,82], especially of side chain bands (e.g., $\nu_s(COO^-)$), and decoupling of the amide I, I′ overall band from $\nu_{as}(COO^-)$ (≈ 1580 cm^{-1}) and amide II could increase the accuracy of dichroic ratios. A complete line shape analysis of the amide I, I′ of Na^+/K^+-ATPase in suspended membrane fragments was performed by Brazhnikov et al. [28]. However, their results are not free of ambiguities since a number of assumptions had to be introduced into the analysis. The non exchanging core of the Na^+/K^+-ATPase was reported to consist of 45% of the amide groups, whereas a value of 24% was obtained in this paper. The corresponding conclusion that 55% of the protein assumes a random structure is questionable since NH groups involved in ordered secondary structures may also undergo H^+/D^+ exchange in short time periods provided the corresponding ordered segments are flexible enough [83,84]. The multistep procedure for line shape analysis used by Brazhnikov et al. consisted in a subtraction of simulated side chain contributions, followed by the subtraction of a synthetic amide I′ band representing 55% of random structure. Finally, a conventional line shape analysis was performed with the remaining 45% of the amide I band, resulting in 20% of α-helix and 25% of antiparallel β-structure. The half-width of the latter component, however, is too large for a regular (nonflexible) structure [85]. It cannot be excluded that this component is a superposition of N-deuterated and N-protonated β-structures. For a reliable analysis, the use of accurate difference spectra in addition to the original spectra is a prerequisite.

Conclusion

The main result of this paper is the demonstration that membrane fragments containing Na^+/K^+-ATPase bind to a lipid bilayer on a germanium plate and that this system may be used for infrared spectroscopic studies of the protein. At a coverage of the lipid surface corresponding to 30–40% of a monolayer of membrane fragments, characteristic infrared bands of the protein such as the amide I and II bands can be clearly resolved. Evidence for orientation of the protein with respect to the supporting lipid layer is obtained from experiments with polarized light, the largest polarization effects being associated with the $-COO^-$ band at 1400 cm^{-1}. Experiments with aqueous media of different ionic composition indicate that the average orientation of transition moments changes when K^+ in the medium is replaced by $Tris^+$ or Na^+. Since ion-specific orientation effects are small and near the detection limit, these results require confirmation by experiments with increased sensitivity.

Acknowledgement

Instrumental support by BRUKER Analytische Meßtechnik, Karlsruhe, F.R.G., is kindly acknowledged. U.P.F. thanks the directorate of the laboratory for Physical Chemistry, ETH Zürich, for facilitating experimental work. This work was financially supported by Deutsche Forschungsgemeinschaft (Sonderforschungsbereich 156).

References

1 Skou, J.C. (1975) Q. Rev. Biophys. 7, 401–434.
2 Robinson, J.D. and Flashner, M.S. (1979) Biochim. Biophys. Acta 549, 145–176.
3 Cantley, L.C. (1981) Curr. Top. Bioenerg. 11, 201–237.
4 Schuurmans Stekhoven, F. and Bonting, S.L. (1981) Physiol. Rev. 61, 1–76.
5 Jørgensen, P.L. (1982) Biochim. Biophys. Acta 694, 27–68.
6 Glynn, I.M. (1985) in The Enzymes of Biological Membranes, 2nd Edn. (Martonosi, A.N., ed.), Vol. 3, pp. 35–114, Plenum Press, New York.
7 Kaplan, J.H. (1985) Annu. Rev. Physiol. 47, 535–544.
8 Forgac, M. and Chin, G. (1985) in Topics in Molecular and Structural Biology Metalloproteins (Harrison, P., ed.), Vol. 2, pp. 123–143, MacMillan, New York.
9 Jørgensen, P.L. (1985) Biochem. Soc. Symp. 50, 59–79.
10 Askari, A. (1987) J.Bioenerg. Biomembr. 19, 359–374.
11 Hiatt, A., McDonough, A.A. and Edelman, I.S. (1984) J. Biol. Chem. 259, 2629–2635.
12 Shull, G.E., Schwartz, A. and Lingrel, J.B. (1985) Nature 316, 6991–695.
13 Shull, G.E., Lane, L.K. and Lingrel, J.B. (1986) Nature 321, 429–431.
14 Ovchinnikov, Yu.A., Modyanov, N.N., Broude, N.E., Petrukhin, K.E., Grishin, A.V., Arzamazova, N.M., Aldanova, N.A., Monastyrskaya, G.S. and Sverdlov, E.D. (1986) FEBS Lett. 201, 237–245.
15 Ovchinnikov, Yu.A., Arzamazova, N.M., Arystarkhova, E.A., Gevondyan, N.M., Aldanova, N.A. and Modyanov, N.N. (1987) FEBS Lett. 217, 269–274.
16 Pachence, J.M., Edelman, I.S. and Schoenborn, B.P. (1987) J. Biol. Chem. 262, 702–709.
17 Mohraz, M., Simpson, M.V. and Smith, P.R. (1987) J. Cell Biol. 105, 1–8.
18 Chin, G.J. (1985) Biochemistry 24, 5943–5947.
19 Nicolas, R.A. (1984) Biochemistry 23, 888–898.
20 Deguchi, N., Jørgensen, P.L. and Maunsbach, A.B. (1977) J. Cell Biol. 75, 619–634.

21 Skriver, E., Maunsbach, A.B. and Jørgensen, P.L. (1981) FEBS Lett. 131, 219–222.

22 Hebert, H., Jørgensen, P.L., Skriver, E. and Maunsbach, A.B. (1982) Biochim. Biophys. Acta 689, 571–574.

23 Zampighi, G., Kyte, J. and Freytag, W. (1984) J. Cell Biol. 98, 1815–1864.

24 Zampighi, G., Simon, S.A., Kyte, J. and Kreman, M. (1986) Biochim. Biophys. Acta 854, 45–57.

25 Grefaldi, T.J. and Wallace, B.A. (1984) J. Biol. Chem. 259, 2622–2628.

26 Dinolfo, T., Gresalfi, T.J. and Wallace, B.A. (1985) in The Sodium Pump (Glynn, I. and Ellory, C., eds.), pp. 63–72, The Company of Biologists Ltd., Cambridge, U.K.

27 Hastings, D.F., Reynolds, J.A. and Tanford, Ch. (1986) Biochim. Biophys. Acta 860, 566–569.

28 Brazhnikov, E.V., Chetverin, A.B. and Chirgadze, Yu.N. (1978) FEBS Lett. 93, 125–128.

29 Chetverin, A.B., Venyaminov, S.Yu., Emelyanenko, V.I. and Burstein, E.A. (1980) Eur. J. Biochem. 108, 149–156.

30 Chetverin, A.B. and Brazhnikov, E.V. (1985) J. Biol. Chem. 260, 7817–7819.

31 Jesaitis, A.J. and Fortes, P.A.G. (1980) J. Biol. Chem. 255, 459–467.

32 Carilli, C.T., Farley, R.A., Perlman, D.M. and Cantley, L.C. (1982) J. Biol. Chem. 257, 5601–5606.

33 Chong, P.L.G., Fortes, P.A.G. and Jameson, D.M. (1985) J. Biol. Chem. 260, 14484–14490.

34 Lee, J.A. and Fortes, P.A. (1986) Biochemistry 25, 8133–8141.

35 Grisham, C.M. and Hutton, W. (1978) Biochem. Biophys. Res. Commun. 81, 1406–1411.

36 Grisham, C.M. (1979) Biochem. Biophys. Res. Commun. 88, 229–236.

37 Grisham, C.M. (1979) in Advances in Inorganic Biochemistry (Eichhorn, G. and Marzilii, L., eds.), pp. 193–218, Elsevier, Amsterdam.

38 O'Connor, S.E. and Grisham, C.M. (1980) FEBS Lett. 118, 303–307.

39 Klevickis, C. and Grisham, C.M. (1982) Biochemistry 21, 69–79.

40 Grisham, C.M. (1982) in Membranes and Transport (Martonosi, A.N., ed.), Vol. 1, pp. 585–592, Plenum Press, New York.

41 Jørgensen, P.L. (1974) Meth. Enzymol. 32, 277–290.

42 Fringeli, U.P. and Günthard, H.H. (1980) in Molecular Biology, Biochemistry and Biophysics, Membrane Spectroscopy (Grell, E., ed.), Vol. 31, pp. 270–332, Springer Verlag, Berlin.

43 Harrick, N.J. (1967) Internal Reflection Spectroscopy, Wiley Interscience, New York.

44 Fringeli, U.P. (1989) in Biologically Active Molecules (Schlunegger, U.P., ed.), pp. 241–252, Springer Verlag, Berlin.

45 Fendler, K., Grell, E., Haubs, M. and Bamberg, E. (1985) EMBO J. 4, 3079–3085.

46 Borlinghaus, R., Apell, H.-J. and Läuger, P. (1987) J. Membrane Biol. 97, 161–178.

47 Takenaka, T., Nogami, K., Gotoh, H. and Gotoh, R. (1971) J. Colloid Interface Sci. 35, 395–402.

48 Fringeli, U.P., Müldner, G.G., Günthard, H.H., Gasche, W. and Leuzinger, W. (1972) Z. Naturforsch. 27b, 780–796.

49 Kopp, F., Fringeli, U.P., Mühlethaler, K. and Günthard, H.H. (1975) Biophys. Struct. Mech. 1, 75–96.

50 Baumeister, W., Fringeli, U.P., Hahn, H., Kopp, F. and Seredynski, J. (1976) Biophys. J. 16, 791–810.

51 Fringeli, U.P. (1977) Z. Naturforsch. 32c, 20–45.

52 Fringeli, U.P. (1980) Biophys. J. 34, 173–187.

53 Brandenburg, K. and Seydel, U. (1985) Biochim. Biophys. Acta 775, 225–238.

54 Naumann, D., Schultz, C., Born, J., Rogge, F. and Labischinski, H. (1988) Microchim. Acta (Wien) I, 379–383.

55 Loeb, G.I. and Baier, R.E. (1988) J. Colloid Interface Sci. 27, 38–45.

56 Baumeister, W., Fringeli, U.P., Hahn, M. and Seredynski, J. (1976) Biochim. Biophys. Acta 453, 289–292.

57 Fromherz, P., Peters, J., Müldner, H.G. and Otting, W. (1972) Biochim. Biophys. Acta 274, 644–648.

58 Hofer, P. and Fringeli, U.P. (1979) Biophys. Struct. Mech. 6, 67–80.

59 Fringeli, U.P., Leutert, P., Thurnhofer, H., Fringeli, M. and Burger, M.M. (1986) Proc. Natl. Acad. Sci. USA 83, 1315–1319.

60 Fringeli, U.P. and Fringeli, M. (1979) Proc. Natl. Acad. Sci. USA 76, 3852–3856.

61 Fringeli, U.P. (1980) J. Membr. Biol. 54, 203–212.

62 Gremlich, H.-U., Fringeli, U.P. and Schwyzer, R. (1983) Biochemistry 22, 4257–4264.

63 Gremlich, H.-U., Fringeli, U.P. and Schwyzer, R. (1984) Biochemistry 23, 1808–1810.

64 Fringeli, U.P. and Hofer, P. (1980) Neurochem. Int. 2, 185–192.

65 Fringeli, U.P., Ahlström, P., Vincenz, C. and Fringeli, M. (1985) SPIE Fourier and Computerized Infrared Spectroscopy 553, 234–235.

66 Fringeli, U.P. (1985) Nachr. Chem. Tech. Lab. 33, 708–711.

67 Schöpflin, M., Fringeli, U.P. and Perlia, X. (1987) J. Am. Chem. Soc. 109, 2375–2380.

68 Kellner, R. and Götzinger, G. (1984) Microchim. Acta (Wien) II, 61–74.

69 Nocentini, M., Gendreau, R.M. and Chittur, K.K. (1988) Microchim. Acta (Wien) I, 343–347.

70 Hutson, T.B., Chang, M.J.W., Keller, J.T. and Long, D.J. (1988) Microchim. Acta (Wien) I, 339–341.

71 Schwartz, A., Nagano, K., Nakao, M., Lindenmayer, G.E. and Allen, J.C. (1971) Meth. Pharmacol. 1, 361–388.

72 Lowry, O.H., Rosebrough, N.J., Farr, A.L. and Randall, R.J. (1951) J. Biol. Chem. 193, 265–275.

73 Blodgett, K.B. and Langmuir, I. (1937) Phys. Rev. 51, 964–982.

74 Fringeli, U.P. (1989) Chem. Phys. Lett., submitted.

75 Suits, G.H. (1978) in The Infrared Handbook (Wolfe, W.L. and Zissis, G.J., eds.), Chapter 3, pp. 1–154, Office of the Naval Research Department of the Navy, Washington, DC.

76 Karlish, S.J.D. and Yates, D.W. (1976) Biochim. Biophys. Acta 527, 115–130.

77 Jørgensen, P.L. and Petersen, T. (1982) Biochim. Biophys. Acta 705, 38–47.

78 Fraser, R.D.B. and MacRae, T.P. (1973) Conformations in Fibrous Proteins and related Synthetic Polypeptides. Chapter 5, Academic Press, New York.

79 Maunsbach, A.B., Skriver, E., Herbert, H. and Jørgensen, P.L. (1983) Curr. Top. Membr. Transp. 19, 123–126.

80 Läuger, P. and Apell, H.-J. (1986) Eur. Biophys. J. 13, 309–321.

81 Apell, H.-J., Borlinghaus, R. and Läuger, P. (1987) J. Membr. Biol. 97, 179–191.

82 Rüegg, M., Metzger, V. and Susi, H. (1975) Biopolymers 14, 1465–1471.

83 Miller, W.G. (1973) Macromolecules 6, 100–107.

84 Ikegami, A., Yamamoto, S. and Oosawa, F. (1965) Biopolymers 3, 555–566.

85 Chirgadze, Yu.N. and Nevskaya, N.A. (1976) Biopolymers 15, 607–625.

86 Seelig, J. and Seelig, A. (1980) Q. Rev. Biophys. 13, 19–61.